INFECTION AND IMMUNITY, Jan. 2009, p. 274–285 Vol. 77, No. 1
0019-9567/09/$08.00+0 doi:10.1128/IAI.00515-08

Four Superoxide Dismutases Contribute to *Bacillus anthracis* Virulence and Provide Spores with Redundant Protection from Oxidative Stress▽†

Robert J. Cybulski, Jr.,[1] Patrick Sanz,[1] Farhang Alem,[1] Scott Stibitz,[2] Robert L. Bull,[3]‡ and Alison D. O'Brien[1]*

Department of Microbiology and Immunology, Uniformed Services University of the Health Sciences, Bethesda, Maryland 20814-4799[1]; FDA CBER, Division of Bacterial, Parasitic and Allergenic Products, NIH Campus Building 29, Room 201, HFM-440, Bethesda, Maryland 20892[2]; and Naval Medical Research Center, 503 Robert Grant Avenue, Silver Spring, Maryland 20910[3]

Received 25 April 2008/Returned for modification 22 June 2008/Accepted 16 October 2008

The *Bacillus anthracis* genome encodes four superoxide dismutases (SODs), enzymes capable of detoxifying oxygen radicals. That two of these SODs, SOD15 and SODA1, are present in the outermost layers of the *B. anthracis* spore is indicated by previous proteomic analyses of the exosporium. Given the requirement that spores must survive interactions with reactive oxygen species generated by cells such as macrophages during infection, we hypothesized that SOD15 and SODA1 protect the spore from oxidative stress and contribute to the pathogenicity of *B. anthracis*. To test these theories, we constructed a double-knockout (Δ*sod15* Δ*sodA1*) mutant of *B. anthracis* Sterne strain 34F2 and assessed its lethality in an A/J mouse intranasal infection model. The 50% lethal dose of the Δ*sod15* Δ*sodA1* strain was similar to that of the wild type (34F2), but surprisingly, measurable whole-spore SOD activity was greater than that in 34F2. A quadruple-knockout strain (Δ*sod15* Δ*sodA1* Δ*sodC* Δ*sodA2*) was then generated, and as anticipated, spore-associated SOD activity was diminished. Moreover, the quadruple-knockout strain, compared to the wild type, was attenuated more than 40-fold upon intranasal challenge of mice. Spore resistance to exogenously generated oxidative stress and to macrophage-mediated killing correlated with virulence in A/J mice. Allelic exchange that restored *sod15* and *sodA1* to their wild-type state restored wild-type characteristics. We conclude that SOD molecules within the spore afford *B. anthracis* protection against oxidative stress and enhance the pathogenicity of *B. anthracis* in the lung. We also surmise that the presence of four SOD alleles within the genome provides functional redundancy for this key enzyme.

Bacillus anthracis, the etiological agent of anthrax, is a gram-positive, nonmotile, spore-forming, rod-shaped, facultatively anaerobic bacterium. The versatility provided by sporulation and facultative vegetative growth demands that *B. anthracis* be equipped to protect both life stages from oxygen radicals, such as those encountered by spores in the environment and those generated endogenously in vegetative cells during the course of aerobic vegetative growth. Furthermore, as a pathogen, *B. anthracis* confronts hostile conditions during infection, such as the oxidative burst of professional phagocytes that take up spores and the various oxidative environments encountered by vegetative cells. Antioxidant enzymes such as superoxide dismutases (SODs), catalases, and peroxidases are primary defense mechanisms utilized by bacteria for preventing oxidative damage (49) and are all present in multiple copies in the *B. anthracis* genome. Along with the small acid-soluble proteins that protect spore-encased DNA from oxygen radicals and other forms of stress (46), some or all of these enzymes may play a role in combating the stresses faced by the two distinct life cycles of *B. anthracis*. Here, we investigate the contribution made by spore-bound SODs to *B. anthracis* oxidative stress defenses.

SODs are enzymes that catalyze the dismutation of the reactive oxygen species (ROS) superoxide anion (O_2^-) to hydrogen peroxide and molecular oxygen (34). These enzymes effectively scavenge O_2^- anions before they are able to cause cellular damage either directly or through the generation of more reactive species such as hydroxyl radicals or peroxynitrite (19). SOD was first discovered and characterized in the 1960s by McCord and Fridovich (34). Since their discovery, SODs have been found in almost all aerobes studied as well as in many anaerobes. SODs have been shown to exhibit high levels of conservation and to fall within three main structural classes based upon metal specificity: copper-zinc, manganese or iron, or nickel. Whereas the documented distribution of nickel SODs within the bacterial community is thus far relatively limited (36), many bacterial species possess SODs of both Cu-Zn and Mn/Fe classes, perhaps due to specialized roles filled by each class. The fact that superoxide anions do not cross nonpolar lipid membranes and the observation that Cu-Zn SODs localize typically to the periplasm, whereas Mn/Fe SODs localize to the cytoplasm, suggest that different SODs have distinct roles in combating exogenously and endogenously produced oxygen radicals, respectively (33, 48). SODs of each class have been implicated as being contributors to virulence in multiple pathogens including *Salmonella enterica* serovar Typhimurium (20, 21), *Mycobacterium tuberculosis* (18,

* Corresponding author. Mailing address: Department of Microbiology and Immunology, Uniformed Services University of the Health Sciences, 4301 Jones Bridge Road, Bethesda, MD 20814-4799. Phone: (301) 295-3400. Fax: (301) 295-3773. E-mail: aobrien@usuhs.mil.

† Supplemental material for this article may be found at http://iai.asm.org/.

‡ Present address: FBI Laboratory, 2501 Investigation Parkway, Quantico, VA 22135.

▽ Published ahead of print on 27 October 2008.

38), *Staphylococcus aureus* (29), *Streptococcus agalactiae* (40), *Francisella tularensis* (4), *Neisseria meningitidis* (54), *Brucella abortus* (22), and *Enterococcus faecalis* (51). A common element in the infectious course of many of these pathogens is that they are capable of surviving interactions with ROS-generating phagocytic cells such as macrophages (2, 12, 39).

The *B. anthracis* genome contains four genes that encode proteins with conserved SOD domains, including two with putative manganese specificity (BAS4177 [*sodA1*] and BAS5300 [*sodA2*]), one with putative copper-zinc specificity (BAS4777 [*sodC*]), and one with likely iron and/or manganese specificity (BAS1378 [*sod15*]) (37, 41). Amino acid sequence identity between the manganese SODs is approximately 54%, with 75% similarity, whereas comparisons between the manganese-bound SODA1 and the iron-bound SOD15 indicate an identity of 45% and a similarity of 60%. A 135-amino-acid stretch at the N terminus of SOD15 distinguishes the protein from other *B. anthracis* SODs, and BLAST searches do not yield clues regarding possible roles for this unique domain beyond a likely helical secondary structure. Interclass comparisons between the Mn/Fe SODs and the Cu-Zn SODC indicate comparatively little homology, although short regions of similarity do exist.

Previous studies (31, 47) indicated that two SODs, SOD15 and SODA1, are present within the *B. anthracis* exosporium. This redundancy suggests an important role for SODs in the spore, possibly in defending against the macrophage and thus contributing to *B. anthracis* virulence. Passalacqua et al. (37) previously constructed single deletions of each of the four SOD genes and demonstrated that none of the deletions led to a significant attenuation of *B. anthracis* when DBA/2 mice were infected via the intratracheal route, although the deletion of *sodA1* did lead to reduced growth under conditions of oxidative stress and increased sensitivity to endogenously produced superoxide anion in the vegetative state. That report did not investigate SOD activity on the surface of the spore or sensitivity to oxidative stress among spores made from deletion strains. Recently, studies of related *Bacillus* species reported a sensitivity of spores to high oxidative stress of multiple forms (13, 14, 42, 55). These observations raise the possibility that multiple chromosomally encoded SODs provide redundant and combinatorial protection of the spore from oxidative stress and suggest that the protective role for SODs might be fully apparent only upon the deletion of multiple *sod* genes from the *Bacillus* genome. Because of this possibility, we constructed *B. anthracis* Sterne strain 34F2 with multiple *sod* deletions to assess the importance of SODs in *B. anthracis* pathogenicity. We found that spores of a *Bacillus* strain in which all four SOD genes were deleted exhibited enhanced sensitivity to agents of oxidative stress, reduced survival in macrophages, and attenuation upon intranasal challenge of mice.

MATERIALS AND METHODS

Bacterial strains. *B. anthracis* Sterne (toxigenic and unencapsulated; Naval Medical Research Center, Silver Spring, MD) and *sod* gene deletion strains listed in Table 1 were used for in vitro and in vivo experiments.

Preparation of recombinant proteins. Our procedures for the construction of a recombinant *Escherichia coli* strain that expressed recombinant SOD15, SODA1, SODC, SODA2, BxpB, or BclA with an N-terminal six-histidine tag and for purification of that protein by nickel affinity chromatography were described in detail elsewhere previously (6). Briefly, genomic DNA was extracted from *B. anthracis* strains with the Easy-DNA kit (Invitrogen, Carlsbad, CA). NdeI-BamHI or XhoI-BamHI fragments that contained each gene of interest were amplified from the Sterne genome by PCRs using the Expand high-fidelity PCR system (Roche Diagnostics, Indianapolis, IN) in a PTC200 Peltier thermal cycler (MJ Research, Bio-Rad, Hercules, CA). Primer sets designed from the flanking sequences of the targeted gene (National Center for Biotechnology Information [http://www.ncbi.nlm.nih.gov.lrc1.usuhs.edu/entrez/viewer.fcgi?db=nucleotide&val=AE017225]) are listed in Table S1 in the supplemental material. PCR products were purified with the QIAEX II gel extraction kit (Qiagen, Valencia, CA), and the DNA fragments were ligated into expression vector pET15b (Novagen, San Diego, CA). The resulting expression plasmids are listed in Table S2 in the supplemental material. DNA sequences were verified with the ABI Prism Big Dye method (Applied Biosystems, Forest City, CA) by the Biomedical Instrumentation Center at the Uniformed Services University, and recombinant plasmids were then transformed into *E. coli* BL21(DE3)(pLysS) according to the pET system manual (Novagen, San Diego, CA). His-tagged proteins were expressed from transformants and subjected to His-Trap nickel affinity column chromatography with the Akta fast protein liquid chromatography system (GE Healthcare, Piscataway, NJ).

TABLE 1. Bacterial strains used or constructed in this study

Strain	Description	Shorthand description	Reference or source
34F2	Wild-type *Bacillus anthracis*	34F2	48a
ΔBclA	34F2 Δ*bclA*	ΔBclA	6
RJC010	34F2 Δ*sod15*	Δ*15*	This study
RJC020	34F2 Δ*sodA1*	Δ*A1*	This study
RJC050	34F2 Δ*sod15* Δ*sodA1*	Δ*15*Δ*A1*	This study
RJC060	34F2 Δ*sod15* Δ*sodA1* Δ*sodC*	Δ*15*Δ*A1*Δ*A2*	This study
RJC070	34F2 Δ*sod15* Δ*sodA1* Δ*sodA2*	Δ*15*Δ*A1*Δ*C*	This study
RJC080	34F2 Δ*sod15* Δ*sodA1* Δ*sodC* Δ*sodA2*	Δ*15*Δ*A1*Δ*A2*Δ*C*	This study
RJC011	34F2 Δ*bclA* Δ*sod15*	Δ*bclA*Δ*15*	This study
RJC021	34F2 Δ*bclA* Δ*sodA1*	Δ*bclA*Δ*A1*	This study
RJC051	34F2 Δ*bclA* Δ*sod15* Δ*sodA1*	Δ*bclA*Δ*15*Δ*A1*	This study
RJC110	34F2 Δ*sodA1* Δ*sodC* Δ*sodA2*	Res15	This study
RJC120	34F2 Δ*sod15* Δ*sodC* Δ*sodA2*	ResA1	This study
RJC150	34F2 Δ*sodC* Δ*sodA2*	Res15,A1	This study

Immune serum and antibody preparation. Polyclonal antibodies were generated against each recombinant SOD by methods previously described (6). Briefly, rabbits were vaccinated monthly with 50 μg of purified recombinant protein in Freund's complete adjuvant for the first inoculation and Freund's incomplete adjuvant for all subsequent immunizations. Production bleeds were taken and analyzed for specific antibodies beginning at month 5, with final bleeds taken at month 12. Immunoglobulin G (IgG) was purified from each final serum bleed by passage of the sample over a protein G column (Pierce Biotechnology, Rockford, IL). Protein concentrations were determined by a microtiter BCA assay (Pierce Biotechnology, Rockford, IL).

Construction of the SOD knockout and restored strains. The construction of the Δ*bclA* deletion strain was described previously (6). Deletion constructs of the *sod15*, *sodA1*, *sodC*, and *sodA2* genes that were suitable for allelic exchange were created by cloning two NotI-XmaI DNA fragments that contained locus-specific flanking regions into the NotI site of pBKJ236 (27). These fragments were created by PCR with primers listed in Table S1 in the supplemental material. Ligation of the two fragments created a precise deletion of the respective open reading frame from the start to the stop codon, inclusively, with an XmaI site generated at the site of the locus. A complete list of plasmid constructs created and used in this study is provided in Table S2 in the supplemental material. The resulting constructs were used to create *sod* null mutants in *B. anthracis* Sterne strain 34F2 by an allelic exchange procedure described previously (27). In brief, the pBKJ236-based plasmid constructs were transferred into strain 34F2 by conjugation, and integrants were isolated by a shift to a replication-nonpermissive temperature followed by growth at the replication-nonpermissive temperature with continuous selection for erythromycin resistance. A second plasmid,

pSS4332, was then introduced into each integrant by conjugative transfer and selection for kanamycin resistance. Plasmid pSS4332, which represents a modification of previously published methods (27) and performs the functions of the previously described pBKJ233, mediates cleavage within the chromosomally inserted pBKJ236-derived construct, an event that stimulates recombination with a loss of the integrated plasmid and gene replacement in a portion of the erythromycin-sensitive candidates. The resulting knockout strains are summarized in Table 1. The absence of the appropriate SOD loci in the various knockout constructs was demonstrated by PCR (as shown in Fig. 2) with primers listed in Table S1 in the supplemental material. These primers were designed to bind to sequences flanking the region included in each deletion construct described above.

Strains hereafter referred to as "restorants" were constructed with the 34F2 Δ*sod15* Δ*sodA1* Δ*sodC* Δ*sodA2* quadruple-knockout strain as the parent and represent the restoration of *sod* genes by allelic exchange. Constructs of the intact *sod15* and *sodA1* loci suitable for allelic exchange were created by the generation of DNA fragments that contained the intact locus, inclusive of flanking regions, from *B. anthracis* Sterne strain 34F2 by PCR with primers listed in Table S1 in the supplemental material. Each PCR-amplified fragment was then cloned into the NotI site of pBKJ236. The allelic exchange was then conducted in two sequential steps as described above for the generation of knockout strains. The restoration of the two *sod* loci was demonstrated by PCR (shown in Fig. 2) with primers listed in Table S1 in the supplemental material.

Generation and purification of *B. anthracis* spores. Single colonies of *B. anthracis* Sterne strain 34F2 or mutant strains were taken from brain heart infusion (BHI) agar plates and inoculated into BHI broth for culture overnight at 37°C. Each culture was spread onto modified germination (G) medium (30) agar plates [0.2% yeast extract, 0.2% $(NH_4)_2SO_4$, 1.5% Bacto agar, 0.0025% $CaCl_2$ dihydrate, 0.05% K_2HPO_4, 0.02% $MgSO_4$ heptahydrate, 0.005% $MnSO_4$ quatrahydrate, 0.0005% $ZnSO_4$ dihydrate, 0.0005% $CuSO_4$ pentahydrate, 0.00005% $FeSO_4$ heptahydrate]. The plates were incubated at 30°C for 10 to 14 days in the dark. Colonies scraped from the surface of the agar were resuspended in distilled water, washed twice in distilled water, and heat treated at 65°C for 1 h to kill any viable vegetative cells. Purification of spores was done with 58% (vol/vol) Renografin (Renocal-76 diluted in distilled water; Bracco Diagnostics, Princeton, NJ). Spores were layered onto 58% Renografin and centrifuged at 6,000 × *g* for 60 min in a swinging bucket rotor. The sedimented spores were washed twice with distilled water. After the final sedimentation, the spores were resuspended in distilled water to yield a final concentration of 10^9 to 10^{10} CFU/ml, as determined by vegetative outgrowth on BHI plates.

Preparation of spore surface protein extract (SSPE). Analysis of the proteins contained within the exosporium was achieved by the removal of the exosporium from whole spores via chemical extraction according to a method described previously (1). Briefly, 0.5 ml of heat-activated spores (10^9 to 10^{10} CFU/ml) was pelleted at 7,000 × *g* for 15 min at 4°C. Spores were washed twice with water and resuspended in 0.5 ml of extraction buffer that contained 0.1 M dithiothreitol, 0.1 M NaCl, and 0.5% sodium dodecyl sulfate (pH 10). Samples were incubated in a 37°C shaking water bath for 2.5 h and pelleted, and the resulting supernatant was collected. Supernatants were then filtered through a 0.2-μm Corning filter and dialyzed against phosphate-buffered saline (PBS).

Western blot analysis of SSPE. The presence of individual SODs within SSPE generated from various *B. anthracis* strains was detected by Western blot analysis. Twenty microliters of SSPE was loaded onto and separated on 4 to 20% Tris-glycine sodium dodecyl sulfate-polyacrylamide gels (Invitrogen, Carlsbad, CA), transferred onto Optitran BA-S 83 reinforced nitrocellulose (Whatman GmbH, Dassel, Germany), and blocked overnight at 4°C in PBST (PBS with 0.5% Tween 20) with 5% nonfat dry milk. Purified His-tagged recombinant proteins were used as positive controls for antibody recognition, with 80 ng of SOD15, 4 ng of SODA1, 100 ng of SODA2, 25 ng of SODC, or 100 ng of BclA loaded where appropriate. The nitrocellulose was then incubated with polyclonal anti-spore protein IgG diluted 1:500 in PBST with 5% nonfat dry milk for 1 h at room temperature. Following three 5-min washes at room temperature with PBST, the nitrocellulose was incubated for 1 h at room temperature with goat anti-rabbit IgG conjugated to horseradish peroxidase (Bio-Rad, Hercules, CA) diluted 1:10,000 in PBST. Blots were then washed three times for 5 min each in PBST and developed with Lumigen PS-3 Acridan (GE Healthcare UK, Buchinghamshire, United Kingdom) and Kodak (Rochester, NY) BioMax XAR film.

Characterization of *B. anthracis sod* mutants and restored strains. Vegetative growth patterns of the parent *B. anthracis* Sterne strain, knockout strains, and restorant strains were determined by the inoculation of BHI agar with cultures grown overnight and measurement of the optical density at 600 nm (OD_{600}) at various times over 8 to 10 h. For all strains, starting inocula registered an OD_{600} of between 0.065 and 0.070, values that corresponded to between 1.00×10^7 and 1.25×10^7 CFU/ml. These data are available in Table S3 in the supplemental material. The growth rate of each strain was measured in three independent experiments. Alternatively, 5×10^8 heat-inactivated spores of each strain were inoculated into 73 ml of preheated modified G medium in a 250-ml Erlenmeyer flask. This inoculation yielded a starting OD_{600} of between 0.040 and 0.051, readings that corresponded to between 3.11×10^6 and 3.90×10^6 CFU/ml. These data are also presented in Table S3 in the supplemental material. The cultures were then grown at 37°C with shaking at 250 rpm, and the OD_{600} was measured at various times over 8 to 10 h. The growth rate of each strain was measured in three independent experiments. Germination efficiencies of the strains were compared by culturing spores in 5% BHI broth, taking samples from the broth cultures at various times, and heat inactivating the vegetative cells at 68°C for 1 h, as previously described (6). The heat-treated broth cultures were then subcultured onto BHI agar to enumerate the residual heat-resistant spores. The decline in heat-resistant CFU over time was tested for each strain in three independent experiments. Within each experiment, three samples of each strain were heat treated and counted, and the geometric mean CFU for like samples was determined. For each of these assays, error bars represent variations among three like samples at each time point ±1 standard deviation.

Measurement of SOD activity in vitro. The SOD activity of each of the four recombinant SODs or recombinant spores was determined with the SOD Assay Kit-WST (Dojindo Molecular Technologies, Gaithersburg, MD) (16). In this assay, superoxide anions generated from the oxidation of xanthine by xanthine oxidase (XO) react with colorless water-soluble tetrazolium salt (WST) to generate a yellow compound, WST-1 formazan (observed spectrophotometrically at 450 nm). This reaction is inhibited in a competitive fashion when superoxide anions are degraded by active SOD. We measured SOD activity as the percent inhibition of WST-1 formazan formation when 2 μg of recombinant SOD protein or between 1.0×10^8 and 1.0×10^9 heat-activated spores in a total volume of 30 μl were mixed with 200 μl of WST working solution (containing WST and xanthine) and 20 μl of XO working solution. Samples were incubated for 20 min at 37°C. To measure the SOD activity associated with whole spores, samples were clarified by centrifugation at 13,200 × *g* for 5 min at 4°C, and the OD_{450} of the supernatant was determined. The percent inhibition of the reaction was calculated by comparing the values to positive (no oxidation of WST in the absence of XO) and negative (no inhibition of WST oxidation in the absence of sample or the use of an irrelevant protein sample) controls. Percent inhibition values were then converted to units of activity from a standard curve (Fig. 1A) that was generated from a recombinant SOD of known specific activity (manganese-containing *E. coli* SOD; Sigma-Aldrich, St. Louis, MO). For this mathematical conversion, an equation that describes the steady-state region of the standard curve (i.e., the slope of the dashed line depicted in Fig. 1A) was used. Results represent the means of three assays, and the error bars indicate ±1 standard deviation.

Test of inhibitory effect of anti-SOD antibodies on spore-associated SOD activity. The impact of polyclonal anti-SOD antibodies on spore-associated SOD activity was evaluated by means of the SOD Assay Kit-WST. For that purpose, samples of 2.5×10^8 heat-activated spores were sedimented by centrifugation and resuspended in 50 μl of PBS that contained 100 μg of appropriate anti-SOD polyclonal IgG. Spore-antibody mixtures were incubated for 24 h at 4°C while shaking. Spores were then washed once in PBS to remove unbound antibody and suspended in a final volume of 30 μl. SOD activity was determined with the kit as described above.

Assessment of sensitivity of vegetative bacilli to endogenously generated oxidative stress. The SOD activity of vegetative bacilli was determined by an agar plate assay as previously described (37), with modifications. Briefly, 200-μl aliquots of 2.5×10^7 CFU/ml heat-activated spores were added to 2.8 ml of 0.7% sterile soft BHI agar. The 3-ml suspension was then spread onto BHI plates. Sterile paper disks (6 mm in diameter) permeated with 10 μl of 5% paraquat (PST-740; Ultra Scientific) dissolved in water were placed atop the solidified soft agar layer. Paraquat is a commercially used herbicide which interacts with the redox pathway of respiring cells and undergoes cyclic reduction-oxidation, a process which generates superoxide anion as a by-product. Given that superoxide anions do not diffuse across lipid membranes, the use of paraquat enables an assessment of the level of SOD protection available within vegetative bacilli. The plates were then incubated overnight at 37°C. The sensitivity of bacilli to endogenous superoxide anions generated from paraquat was measured as the area (in mm^2) of growth inhibition around the disk. For each experiment, 10 disks (2 disks per plate) were used.

Evaluation of spore sensitivity to exogenously generated oxidative stress. Spore survival in the presence of exogenously generated superoxide anion was tested by methods described previously (22). Briefly, heat-activated spores were washed twice with PBS (pH 7.5) and resuspended at a final concentration of 5 ×

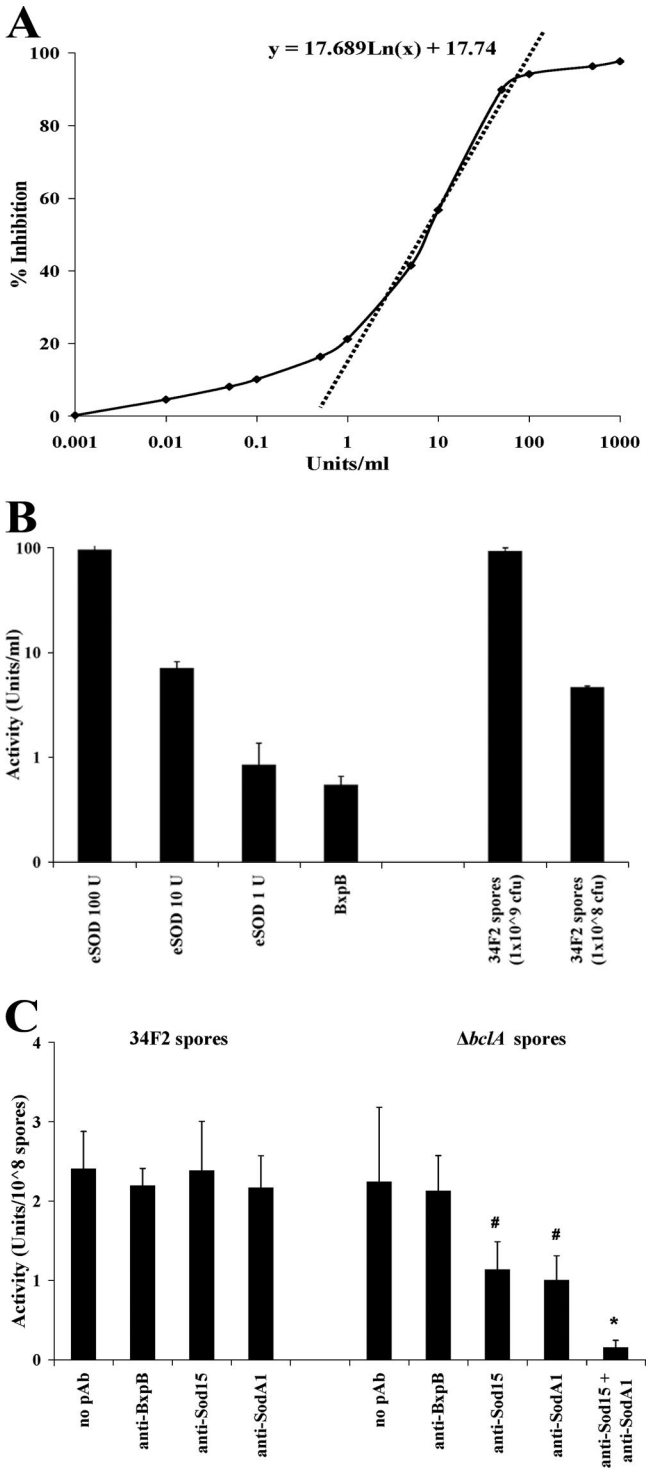

FIG. 1. Demonstration of spore-associated SOD activity. (A) SOD activity was measured spectrophotometrically with the Dojindo SOD Activity Kit-WST. Activity in that kit is expressed as the percent inhibition of the XO-mediated conversion of colorless WST-1 to yellow WST formazan, as described in Materials and Methods. We then used an *E. coli* manganese SOD (eSOD) of known specific activity to generate a standard curve from which to convert percent inhibition to units of SOD activity. For this mathematical conversion, an equation that describes the steady-state region of the standard curve (i.e., the slope of the dashed line depicted in the figure) was used and is presented. (B) Spore-associated SOD activity was assessed using 2.5×10^9 or 2.5×10^8 34F2 spores. *E. coli* manganese SOD of known specific activity was used as a positive control. An irrelevant *B. anthracis* exosporium protein (2 μg of His-tagged, purified BxpB) was included as a negative control. (C) 34F2 and Δ*bclA* spore-bound SOD activity (percent inhibition) in the presence of anti-SOD or control (anti-BxpB) antibodies. ∗, incubation with α-SOD15 plus α-SODA1 polyclonal antibodies yielded a statistically significant decline in measurable SOD activity ($P = 0.004$); #, incubation with α-SOD15 or α-SODA1 alone failed to yield a statistically significant decreases ($P \geq 0.087$).

10^6 CFU/ml in PBS with xanthine at a final concentration of 1 mM, along with 0.5 units of XO and 1,000 units of catalase dissolved in 50 mM potassium phosphate (pH 7.5). Spores were incubated at 37°C, and spore viability was assessed at 0, 15, 30, and 60 min by colony counts of serial 10-fold dilutions of samples plated onto BHI agar. Results were expressed as the percent spore survival measured by comparing spore counts at a given time (t_x) with those present at the initial time (t_0).

Macrophage infection model. The interaction of spores with macrophages of the RAW264.7 cell line (American Type Culture Collection [ATCC], Rockville, MD) was studied by methods detailed previously (28, 53), with modifications. Briefly, the cell line was grown in Dulbecco's minimal essential medium (DMEM) with 10% fetal bovine serum (Lonza, Walkersville, MD). Seed cultures were subcultured onto six-well plates and incubated at 37°C in air with 5% CO_2 for 3 to 4 days until cells reached a density of $(0.8 \text{ to } 1.2) \times 10^6$ cells/well. Cells were washed three times with PBS and infected at 5×10^6 CFU/well with spores suspended in serum-free DMEM that contained 100 ng/ml phorbol 12-myristate 13-acetate (PMA) (8). Cells were incubated at 37°C in air with 5% CO_2 for 45 min. Unphagocytosed spores were then removed by washing the wells three times with PBS. Serum-free DMEM that contained 100 ng/ml PMA and 50 μg/ml gentamicin was added to each well, and cells were incubated at 37°C in air with 5% CO_2 for 45 min to kill extracellular bacteria. The cells were then washed three times with PBS, and fresh serum-free DMEM was added. Cells were incubated at 37°C in air with 5% CO_2 for 0, 2, 4, and 6 h, after which bacterial viability was assessed as follows. At each harvest time, cells were washed three times with PBS and incubated for 5 min in 1 ml of 0.01% bovine serum albumin in water to lyse macrophages. Wells were scraped with a sterile rubber syringe stopper and pipetted into tubes. Lysates were heated at 65°C for 1 h to kill germinated spores before 10-fold serial dilutions were prepared for colony counts on trypticase soy agar plates. The viability of the bacteria was expressed as the percent survival at a given time point (t_x) compared to that for a sample taken at an initial time point (t_0).

Mouse challenge model. The 50% lethal doses (LD_{50}s) of 34F2, mutant strain, and restorant strain spores were determined for both the intranasal and subcutaneous routes of infection. For intranasal spore challenge, mice were sedated with isoflurane with an XGI-8 gas anesthesia system (Xenogen Corporation). Heat-activated spore suspensions of various concentrations (see below) in 25 μl were placed onto the nares of anesthetized mice, and the mice were held upright until the suspension was inhaled (45). Treatment groups of 10 mice received doses of spores that ranged from $\sim 10^3$ to 10^6 34F2 spores and $\sim 10^3$ to 10^7 mutant and restorant strain spores. For subcutaneous spore challenge, 200 μl of each dose of heat-activated spores in suspension was delivered through a tuberculin syringe fitted with a 29-gauge needle into the loose skin beneath the right foreleg of the mouse. Treatment groups of 10 mice for 34F2 challenge and 5 mice for mutant and restorant strain challenges received doses that ranged from $\sim 10^2$ to 10^5 spores.

Statistical evaluations. The vegetative growth curves of the wild-type and mutant strains were generated by plotting the average outcomes (OD_{600}) of three experiments per strain. SOD activity differences were analyzed by one-way analysis of variance (ANOVA) followed by Tukey's pairwise post hoc comparisons. Differences in spore germination rates or percent survival of spores exposed to exogenously generated oxygen radicals or macrophages were appraised by repeated-measures ANOVA followed by one-way ANOVA and Tukey's pairwise post hoc comparisons. The LD_{50} of each selected strain used in these experiments, along with 95% confidence limits, was calculated by probit analysis. Differences in survival and mean time to death (MTD) for an intranasal challenge at 10^6 spores were calculated by Fisher's exact test and Kaplan-Meier analysis, respectively.

RESULTS

Detection of SOD activity within the spore structure. Heat-inactivated whole spores of *B. anthracis* Sterne strain 34F2 were tested for the presence of SOD activity by a commercially available in vitro assay that spectrophotometrically measures the dismutation of superoxide anions. A standard curve (Fig. 1A) generated using a well-characterized *E. coli* SOD of known specific activity allowed the values generated by this assay to be converted into units of enzymatic activity (16). Using these methods, spore-associated SOD activity was detectable (Fig. 1B), as was activity associated with recombinant forms of each of the four SODs encoded by the *B. anthracis* genome (data not shown). While the expression of these recombinant proteins in an artificial system makes it difficult to ensure proper folding and metallation and therefore to make statements about relative levels of activity, the confirmation of some level of activity above background in the presence of each recombinant form indicates that each protein is in fact a functional SOD. In combination with the detection of spore-associated SOD activity and previous data that localized SODs to the *B. anthracis* spore (31, 47), these data support the assertion that SOD15 and SODA1 are active within the spore.

We next tested whether polyclonal IgG raised against SOD15 and SODA1 could inhibit the activity of SODs on the surface of wild-type 34F2 spores and spores of an isogenic *bclA* mutant from which the outer hair-like nap was no longer expressed (see reference 6 for a description of the properties of that strain). Although these anti-SOD antibodies had no effect on SOD activity found on the surface of wild-type 34F2 spores, most likely due to the barrier effect of BclA on the outer surface of the exosporium, they were capable of reducing activity in the presence of Δ*bclA* spores (Fig. 1C). Moreover, the inhibitory effect of each individual anti-SOD antibody was additive, as indicated by the greater total inhibition noted upon the simultaneous incubation of Δ*bclA* spores with both anti-SOD15 and anti-SODA1 IgG. These effects were specific, since antibodies against BxpB (a major component of the exosporium exposed in the absence of BclA) (11) did not affect spore-associated SOD activity. These data agree with enzyme-linked immunosorbent assay and immunoelectron microscopy results indicating that anti-SOD antibodies bind specifically to the surface of whole spores in the absence, but not in the presence, of BclA (11) and suggest that the SOD activity associated with the spore is attributable primarily to the spore-bound SOD protein that is localized to the outer layers of the spore and is available for recognition and inhibition.

A *B. anthracis* Δ*sod15* Δ*sodA1* mutant is unattenuated in an A/J mouse model. To examine the contribution of spore-associated SOD activity to the virulence of *B. anthracis*, a Δ*sod15* Δ*sodA1* double mutant with markerless deletions of *sod15* and *sodA1* was generated via homologous recombination by a modified version of a previously described method (27) (Fig. 2). This technique replaced the open reading frame in question with an XmaI site (CCCGGG) and would not be expected to exert polarity on downstream genes. Mutants were compared to the wild type for defects in growth from either cultures grown overnight or heat-inactivated spores (Fig. 3A and B). The Δ*sod15* Δ*sodA1* mutant replicated like wild-type strain 34F2 from a culture grown overnight but showed a slight delay in vegetative cell outgrowth from spores. We speculated that this delay in bacillus growth from Δ*sod15* Δ*sodA1* spores might be attributable to a delay in the germination of those spores. We then tested this hypothesis and found that the Δ*sod15* Δ*sodA1* mutant spores did in fact germinate more slowly than did 34F2 spores (Fig. 3C). Additionally, the growth of the Δ*sod15* Δ*sodA1* mutant was more sensitive to oxidative stress, as shown by the increased zones of inhibition surrounding disks impregnated with the redox cycling compound paraquat compared to that for 34F2 (Fig. 4A). This increased sensitivity of vegetative cells to endogenously produced superoxide anion is consistent with the idea that SODA1 is the predominant protective enzyme during aerobic growth, as was previously reported (37). However, spores made from the Δ*sod15* Δ*sodA1* mutant unexpectedly showed increased levels of SOD activity compared to levels for 34F2 spores (Fig. 4B). Analysis of single Δ*sod15* and Δ*sodA1* spores suggested that the increase in activity was attributable primarily to the deletion of *sod15*, as Δ*sod15* showed an increase in activity similar to that of the double knockout, whereas the Δ*sodA1* strain had levels of activity that resembled those of the wild type (data not shown). Evaluation of the virulence of the Δ*sod15* Δ*sodA1* mutant in the Sterne strain-sensitive A/J mouse model indicated no attenuation compared to the wild type as assessed by both intranasal and subcutaneous LD_{50} values for spore-challenged A/J mice (Table 2 and Fig. 5).

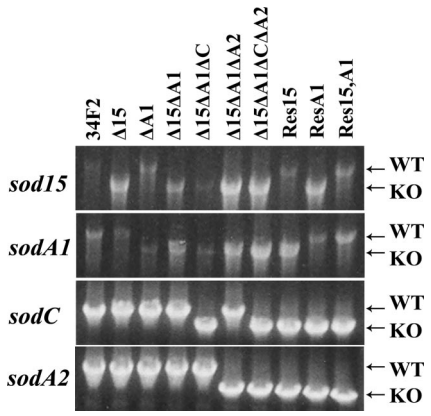

FIG. 2. Deletion of the *B. anthracis* SOD genes. PCRs show the deletion and restoration of genes from the *sod15* (BAS1378), *sodA1* (BAS4177), *sodC* (BAS4777), and *sodA2* (BAS5300) loci. Lower (larger) bands represent intact loci, whereas higher (smaller) bands depict deleted loci in which the gene of interest is deleted and flanking regions are left intact. Primers were designed to bind to sites outside the flanking regions of the targeted loci. Primers used and sizes of PCR fragments generated in these reactions are provided in Table S1 in the supplemental material. Strain shorthand reflects the affected loci of the strain. For example, the Δ*15*Δ*A1* strain possesses deletions (smaller PCR products) at *sod15* and *sodA1* and wild-type (WT) loci (larger PCR products) at *sodA2* and *sodC*, whereas the Res15,A1 strain constructed from the Δ*sod15* Δ*sodA1* Δ*sodC* Δ*sodA2* background possesses restored loci at *sod15* and *sodA1* and deletions at *sodA2* and *sodC*. KO, knockout.

Demonstration of functional redundancy among SOD genes in the *B. anthracis* genome. Western blot analyses of the SSPEs taken from the 34F2 and Δ*sod15* Δ*sodA1* strains indicated that upon the deletion of *sod15* and *sodA1*, at least one of the remaining SODs (SODA2) encoded by the *B. anthracis* ge-

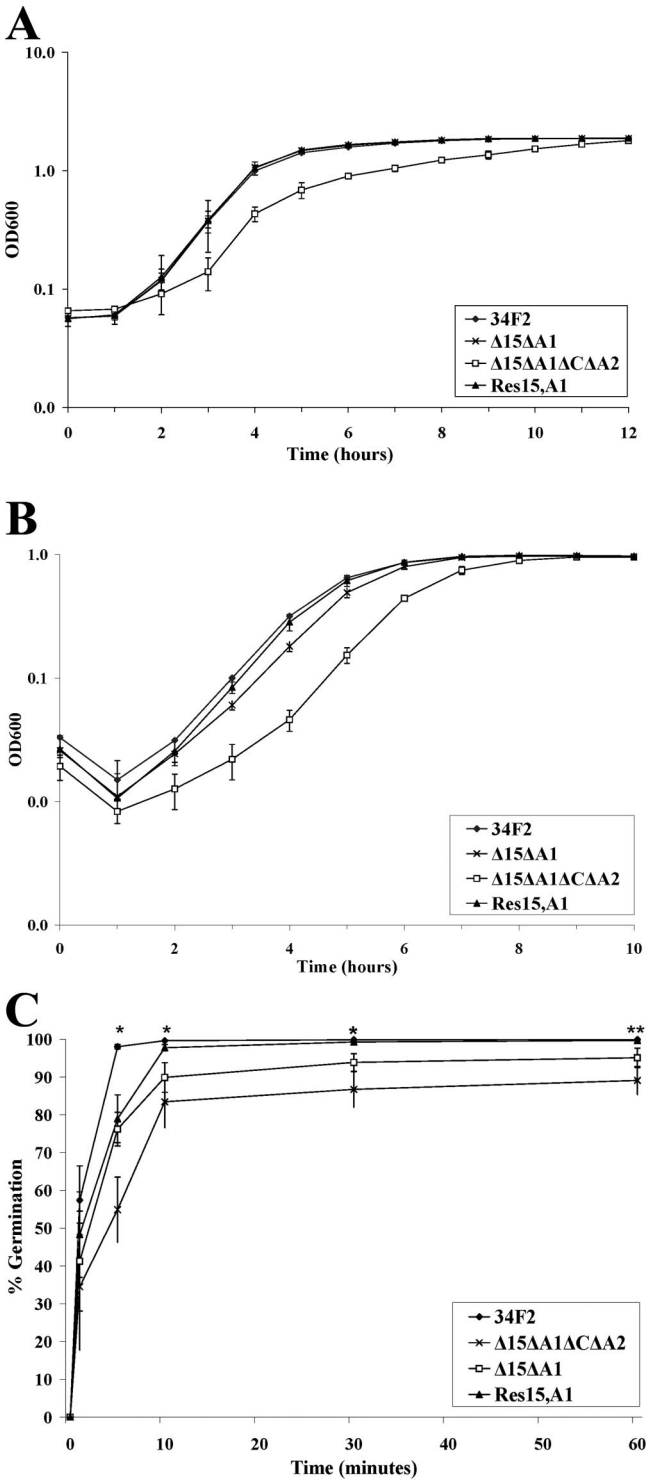

FIG. 3. Growth and germination of *B. anthracis* wild-type and mutant strains. (A) Vegetative growth of the wild-type Sterne strain and SOD deletion mutants in BHI broth over time after inoculation with cultures grown overnight. (B) Vegetative outgrowth of the wild-type Sterne strain and SOD deletion mutants in modified G broth over time after inoculation with 5×10^8 heat-activated spores. (C) Kinetics of germination of spores from the parent and mutant strains. Spores were inoculated in 5% BHI broth and grown at 37°C and 225 rpm, and samples were heat treated to inactivate vegetative cells at the time points shown. Colony counts following heat treatment represent the numbers of heat-resistant spores. Percent germination at test points (t_x) indicate the numbers of spores that germinated at each time point relative to the spore count at the starting point (t_0). *, the levels of germination of Δ*sod15* Δ*sodA1* and Δ*sod15* Δ*sodA1* Δ*sodC* Δ*sodA2* spores were statistically lower than those of the wild type at each time point ($P < 0.001$); **, the level of Res15,A1 germination was lower than that of the wild type at the 5-min ($P < 0.001$), 10-min ($P = 0.002$), and 30-min ($P = 0.007$) time points, but by 60 min, the differences were not significant ($P = 0.10$).

nome was incorporated into the spore (Fig. 6). To better understand the nature of the compensation in spore-associated SOD activity seen with Δ*sod15* Δ*sodA1*, triple- and quadruple-deletion mutations were generated from the Δ*sod15* Δ*sodA1* mutant background (Fig. 2). Analysis of the various deletion strains indicated that whereas the deletion of *sod15* and *sodA1* results in the incorporation of SODA2 into the spore, SODC is incorporated at a detectable level only when all three other *sod* genes have been (Fig. 6). Further analysis demonstrated that each genotype possessed a different amount of spore-bound SOD activity (Fig. 4B). Only upon the removal of all four *sod* genes from the genome was all detectable SOD cleared from the SSPE (Fig. 6), with a corresponding complete elimination of spore-associated SOD activity (Fig. 4B). In addition to being without spore-bound SOD activity, the Δ*sod15* Δ*sodA1* Δ*sodC* Δ*sodA2* strain displayed a delay in spore germination as well as a delay in vegetative outgrowth from both heat-inactivated spores and cultures grown overnight (Fig. 3). Furthermore, vegetative bacilli of the quadruple-knockout strain showed greater sensitivity to paraquat than did 34F2 bacilli (Fig. 5A), although the increase in the area of inhibition beyond that of Δ*sod15* Δ*sodA1* was not statistically significant.

Attenuation of the Δ*sod15* Δ*sodA1* Δ*sodC* Δ*sodA2* strain in the mouse model of intranasal infection. Upon the successful elimination of all spore-bound SOD activity, we attempted to assess the importance of SODs in *B. anthracis* virulence by challenging A/J mice with Δ*sod15* Δ*sodA1* Δ*sodC* Δ*sodA2* spores (45). Mice were infected by both the subcutaneous and intranasal routes to examine possible differences in the relative importances of oxidative stress resistance for each infectious route (Table 2). Subcutaneous infection revealed a nonsignificant difference in LD_{50}s between 34F2 (1.13×10^3 CFU) and the Δ*sod15* Δ*sodA1* Δ*sodC* Δ*sodA2* strain (5.04×10^3 CFU) of less than fivefold, whereas intranasal challenge showed a variation between 34F2 (5.57×10^4 CFU) and the Δ*sod15* Δ*sodA1* Δ*sodC* Δ*sodA2* strain (2.51×10^6 CFU) of more than 40-fold. While the Δ*sod15* Δ*sodA1* Δ*sodC* Δ*sodA2* strain appeared to be attenuated by both routes, only the difference in LD_{50}s seen by intranasal inoculation was statistically significant ($P < 0.005$), as assessed by probit analyses.

Enhanced susceptibility of *B. anthracis* Δ*sod15* Δ*sodA1* Δ*sodC* Δ*sodA2* spores to exogenous oxidative stress. The attenuation of the Δ*sod15* Δ*sodA1* Δ*sodC* Δ*sodA2* strain in mice is suggestive of a role for spore-associated SODs in *B. anthracis* pathogenesis. The most obvious role for SODs bound within the spore structure would be to protect against sources of oxidative stress during the early stages of infection. To better understand the relationship between spore-associated SOD activity and resistance to oxidative stress, spores were subjected to exposure to exogenously generated superoxide anions

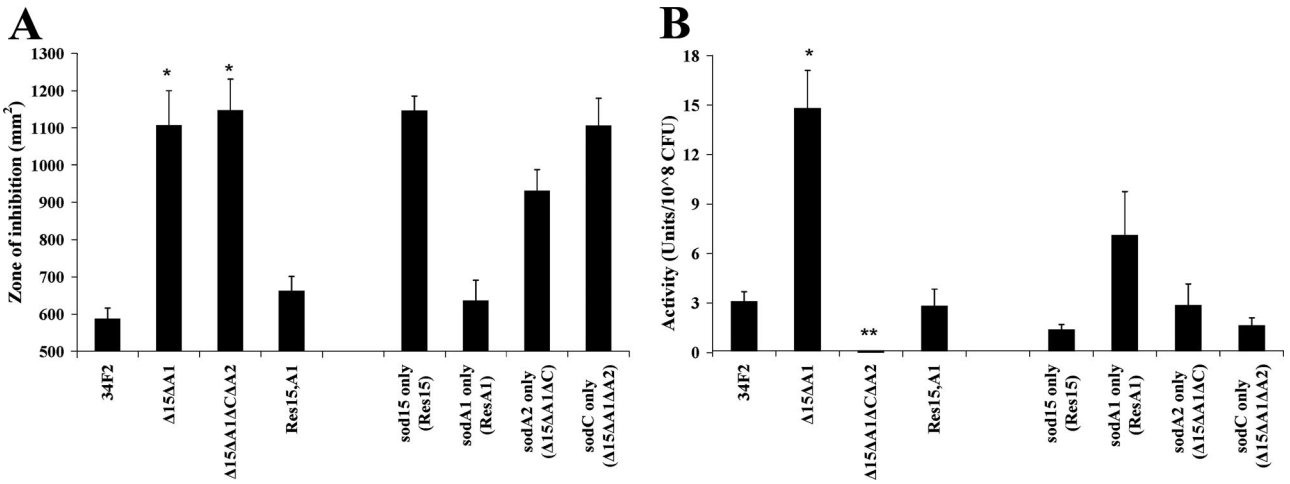

FIG. 4. Comparison of SOD activities for the wild-type Sterne strain and mutants. (A) A total of 2.5×10^7 heat-activated spores were mixed with soft agar and spread onto BHI agar, and plates were overlaid with 6-mm disks soaked with paraquat. After overnight incubation of the plates at 37°C, zones of inhibition of bacterial growth around the disk were calculated as the area (mm^2) of the disk in which bacterial growth was interrupted ($n = 10$ disks per strain per experiment). *, zones of inhibition were higher than those for the wild type ($P < 0.001$). (B) Spore-associated SOD activity from 2.5×10^8 heat-activated spores was measured. *, SOD activity was higher than that of wild-type spores ($P < 0.001$); **, SOD activity was lower than that of wild-type spores ($P < 0.001$).

(Fig. 7). These superoxide anions were supplied from the oxidation of the compound xanthine by XO. The Δ*sod15* Δ*sodA1* Δ*sodC* Δ*sodA2* mutant spores displayed greater sensitivity to oxidative stress than did 34F2 spores, as demonstrated by the decreased percent survival over time (Fig. 7A). The Δ*sod15* Δ*sodA1* mutant spores, which previously demonstrated increased SOD activity compared to that of 34F2, showed a degree of resistance no different from that of 34F2.

Macrophages kill Δ*sod15* Δ*sodA1* Δ*sodC* Δ*sodA2* spores more rapidly than they kill 34F2 spores. Given the observed differences in sensitivity to artificially generated exogenous oxidative stress and the potential role of ROS as contributors to the destruction of *B. anthracis* in macrophages, we next investigated the comparative levels of sensitivity to macrophage killing. 34F2 and *sod* mutant spores were tested for their abilities to survive phagocytosis by RAW 264.7 macrophages. As shown in Fig. 8, phagocytosed Δ*sod15* Δ*sodA1* Δ*sodC* Δ*sodA2* spores were more sensitive to killing by macrophages than either 34F2 or Δ*sod15* Δ*sodA1* spores. The increased level of SOD activity resident in Δ*sod15* Δ*sodA1* spores in comparison to the level in 34F2 spores did not translate into greater survival, as spores of both strains were killed at the same rate.

Restoration of wild-type SOD activity and virulence by restoration of *sod15* and *sodA1*. In order to further demonstrate

TABLE 2. LD_{50} and MTD for intranasal and subcutaneous infections of A/J mice with 34F2 and mutant strains[a]

Strain	LD_{50}[b]		No. of surviving animals/total no. of animals after i.n. challenge with 10^6 CFU	MTD of animals after i.n. challenge with 10^6 CFU
	Intranasal	Subcutaneous		
34F2	5.57×10^4	1.13×10^3	0/10	3.80
Δ*sod15* Δ*sodA1* mutant	4.47×10^4	2.47×10^3	0/10	4.90
Δ*sod15* Δ*sodA1* Δ*sodC* Δ*sodA2* mutant	2.51×10^6*	5.04×10^3	9/10**	6.00***
sod15$^+$ *sodA1*$^+$ restorant	1.28×10^5	3.21×10^3	0/10	4.50

[a] *, statistically significant difference from the wild type, with a P value of <0.005 (the relative median potency of the Δ*sod15* Δ*sodA1* Δ*sodC* Δ*sodA2* strain compared to that of 34F2 was 0.7419, with 95% confidence limits of 0.5103 and 0.9050); **, statistically significant difference from the wild type, with a P value of 0.0001; ***, statistically significant difference from the wild type, with a P value of <0.005 (the 95% confidence limits for wild-type MTD were 3.04 to 4.56 days). i.n., intranasal.

[b] LD_{50}s were calculated and compared by probit analysis.

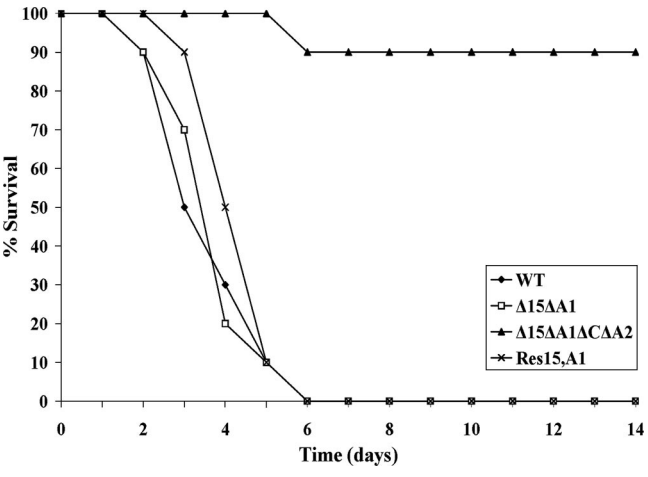

FIG. 5. Percent survival of A/J mice challenged intranasally with 10^6 spores of 34F2, Δ*sod* mutant, and *sod* restorant strains. Treatment groups of 10 mice received 25 μl of a ~4×10^7-CFU/ml heat-activated spore suspension (1×10^6 CFU). Spores were placed onto the nares of anesthetized mice, and the mice were held upright until the suspension was inhaled. Survival of the mice was monitored for a period of 14 days. MTD was significantly different for Δ*sod15* Δ*sodA1* Δ*sodC* Δ*sodA2* spores (6.0 days) compared to that for wild-type (WT) spores (3.80 days) ($P < 0.005$).

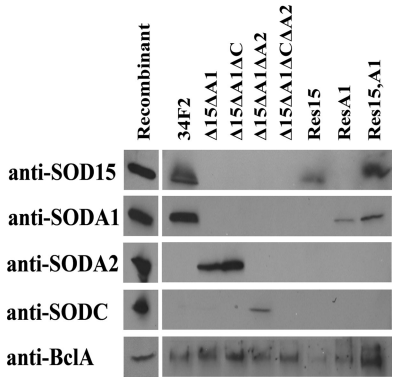

FIG. 6. Detection of individual SODs within spore extracts by Western blot analysis. Shown are data for incubations of SSPEs prepared from 34F2, mutant, or restorant strain spores with anti-SOD polyclonal IgG. Recombinant proteins were included as controls for antibody recognition (see Materials and Methods).

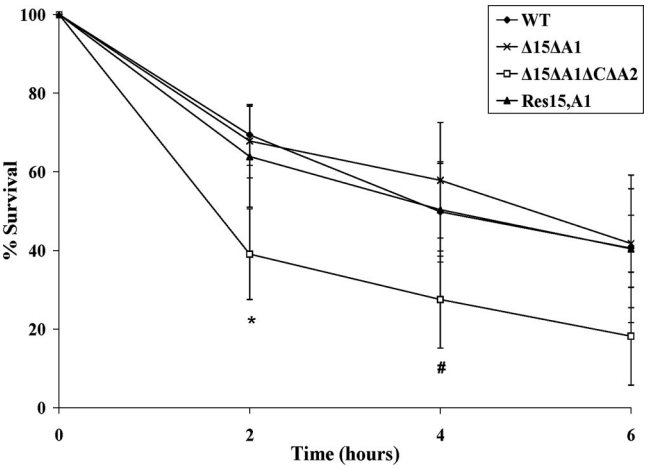

FIG. 8. Resistance of wild-type Sterne strain and SOD deletion mutant spores to macrophage killing. A sample of 5×10^6 heat-activated spores was added to (0.8 to 1.2) $\times 10^6$ RAW264.7 macrophages in serum-free DMEM plus 100 ng/ml PMA. Spore counts were measured at 0, 2, 4, and 6 h by plating onto tryptic soy agar according to procedures described in Materials and Methods. *, percent survival for Δ*sod15* Δ*sodA1* Δ*sodC* Δ*sodA2* spores was less than that for wild-type (WT) spores at 2 h ($P = 0.03$); #, at 4 h, the difference was not statistically significant ($P = 0.08$).

that the phenotypes associated with Δ*sod15* Δ*sodA1* Δ*sodC* Δ*sodA2* were directly related to the absence of SODs in the spore, we next attempted to restore *sod15* and *sodA1* to the quadruple-knockout strain. The "restorants" were generated in a Δ*sod15* Δ*sodA1* Δ*sodC* Δ*sodA2* background by the same markerless replacement techniques used in the *sod* gene deletion strategy (outlined in Materials and Methods). The *sod15*$^+$ *sodA1*$^+$ double restorant (Res15,A1) grew as well as did 34F2, either from cultures grown overnight or from heat-inactivated spores (Fig. 3A and B). The growth kinetics following the inoculation of heat-inactivated spores into growth medium suggested that any initial delay in germination (Fig. 3C) was overcome at later time points and did not significantly hinder vegetative outgrowth. Additionally, Res15,A1 demonstrated wild-type levels of SOD activity both in the vegetative bacilli (Fig. 4A) and on the surface of the spore (Fig. 4B). The LD_{50} of spores of the double restorant introduced both subcutaneously and intranasally into A/J mice was equivalent to that of 34F2 (Table 2), as were the kinetics of infection after an intranasal inoculum of ~10^6 spores (Fig. 5). Finally, in vitro assessments of the sensitivity of Res15,A1 to oxidative stress (Fig. 7) and macrophage killing (Fig. 8) indicated that the restoration of *sod15* and *sodA1* enabled levels of resistance similar to that of 34F2.

DISCUSSION

Here, we describe the construction of a series of *sod* gene deletions in *B. anthracis* that allow an examination of the role played by SODs in the organism's pathogenesis. Proteomic analyses (31, 47) of the *B. anthracis* spore indicated that at least two of the four SODs encoded by the bacterial genome were

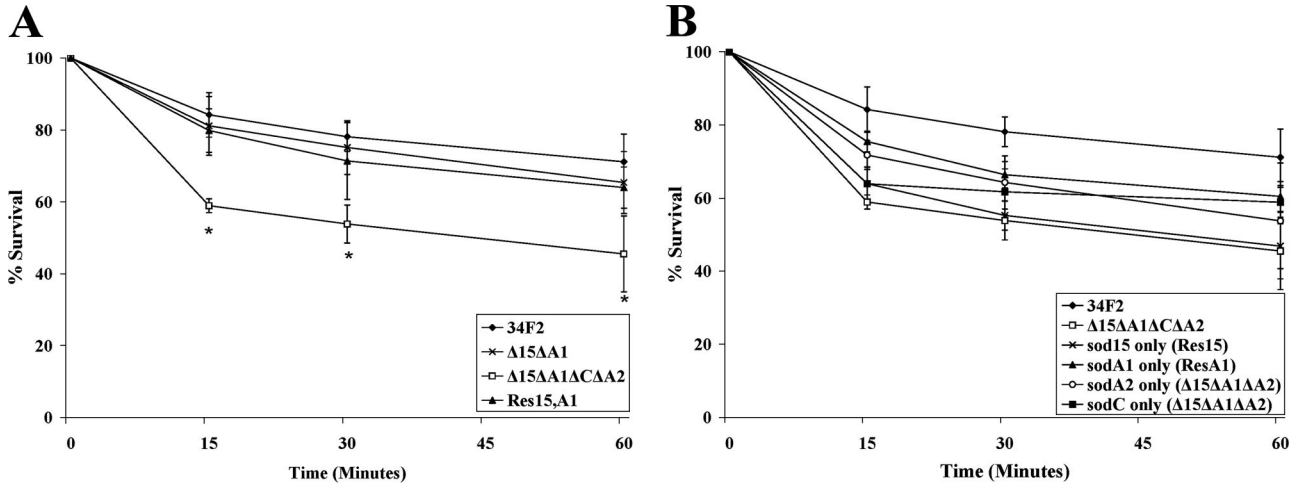

FIG. 7. Resistance of wild-type Sterne strain and SOD deletion mutant spores to oxidative stress. A sample of 5×10^6 heat-activated spores was incubated with 1 mM xanthine, 0.5 units XO, and 1,000 units of catalase at 37°C. Samples were taken at 0, 15, 30, and 60 min. *, percent survival for Δ*sod15* Δ*sodA1* Δ*sodC* Δ*sodA2* spores was less than that for wild-type spores at all time points ($P \leq 0.023$).

present in the endospore. These findings raised the possibility of combinatorial protection from oxidative stress. To test this theory, we constructed a strain that lacked both spore-associated SODs. The Δ*sod15* Δ*sodA1* mutant showed a decrease in resistance to oxidative stress in the vegetative form compared to wild-type strain 34F2, findings that are consistent with results described previously by Passalacqua et al. (37). However, spores generated from the Δ*sod15* Δ*sodA1* strain showed an increase in spore-associated SOD activity. This unanticipated compensation for the loss of *sod15* and *sodA1* was accompanied by the appearance of an alternate SOD species within the spore structure. Furthermore, the Δ*sod15* Δ*sodA1* strain was not attenuated in the A/J mouse model. Additional deletions of the *sodA2* and *sodC* genes produced a Δ*sod15* Δ*sodA1* Δ*sodC* Δ*sodA2* quadruple-knockout strain that displayed a loss of SOD activity associated with the spore. This Δ*sod15* Δ*sodA1* Δ*sodC* Δ*sodA2* strain was attenuated when inoculated intranasally into mice. Additionally, the virulence of the strains correlated with the sensitivity of the organisms to exogenously produced superoxide anion or activated macrophages. The restoration of *sod15* and *sodA1* within the quadruple-knockout background generated a strain (Res15,A1) that essentially mimicked wild-type phenotypes in all aspects related to SOD activity, oxidative stress resistance, and virulence.

This study was founded on the hypothesis that SODs incorporated into the spore structure afford the spore increased resistance to oxidative stress that translates into enhanced virulence through an increased capacity of spores to survive interactions with ROS-producing phagocytes. The data presented in this paper strongly support the notion that the protection from oxidative stress afforded by spore-bound SODs is necessary for the organism to achieve peak virulence, at least within the A/J mouse model. However, alternative explanations for the attenuation seen in the absence of *sod* genes remain possible. One such explanation involves a role for SODs in proper spore formation. Work done by Henriques and colleagues (25) with the related species *Bacillus subtilis* showed that the deletion of the primary bacterial SOD led directly to a change in the spore ultrastructure. Those authors speculated that such structural changes indicate a role for SODs in promoting the appropriate chemistry necessary for proper spore maturation; i.e., the construction of outer spore layers might be dependent on a local redox environment that is affected by the presence or absence of SODs. While those authors reported no discernible effects on spore resistance properties in the face of these ultrastructural differences, and while recent studies by Passalacqua et al. (37) similarly failed to find profound structural changes upon the deletion of any of the SODs encoded by *B. anthracis*, it is formally possible that the deletion of the four *sod* genes of *B. anthracis* may result in changes to the spore structure relevant to stress resistance. In such a situation, the increased sensitivity demonstrated by Δ*sod15* Δ*sodA1* Δ*sodC* Δ*sodA2* spores in the face of exogenous superoxide anion (Fig. 7) and macrophage phagocytosis (Fig. 8) may in fact be an indication of a change in the resistance properties of the spores with respect to multiple forms of stress rather than an increased sensitivity specifically to oxidative stress.

In this investigation, we observed definite changes in both *B. anthracis* growth and germination kinetics that appeared to be directly attributable to the absence of *sod* genes. Perhaps not surprisingly, a delay in the vegetative growth rates of certain mutants correlated with an increased sensitivity of the vegetative bacilli to endogenous oxidative stress. Intermediate knockout and restorant strains that carried *sodA1* or *sodA2* alone exhibited a certain degree of resistance to the effects of paraquat compared to the Δ*sod15* Δ*sodA1* Δ*sodC* Δ*sodA2* strain (Fig. 4A) and displayed wild-type growth characteristics (Fig. 3A). Conversely, strains that carried *sod15* or *sodC* alone showed little capacity to grow vegetatively in the face of endogenous oxidative stress and had growth rates similar to those of the Δ*sod15* Δ*sodA1* Δ*sodC* Δ*sodA2* strain. These differences indicate a specific role for SOD-mediated protection from internal oxidative stress in achieving maximum growth rates.

Germination was also affected by the SODs available to the organism. Both the Δ*sod15* Δ*sodA1* and Δ*sod15* Δ*sodA1* Δ*sodC* Δ*sodA2* strains demonstrated delayed kinetics compared to those of 34F2 (Fig. 3C), although the total extent of germination is ultimately the same for all strains (data not shown). The restoration of the *sod15* and *sodA1* loci within the quadruple-knockout background restored wild-type germination. These results are notable in light of a previous study (3) that suggested the possibility of an interplay between the local redox environment and optimal germination. The findings in that study raise the possibility that the attenuation of our SOD quadruple mutant might be attributable to delayed-germination phenotypes rather than to the role of SODs in oxidative stress resistance. However, several pieces of evidence suggest that slower germination cannot fully explain the reduced virulence of the Δ*sod15* Δ*sodA1* Δ*sodC* Δ*sodA2* strain. The fact that the Δ*sod15* Δ*sodA1* double-deletion strain exhibited wild-type virulence despite slower germination kinetics indicates that a retardation in spore germination does not a priori lead to a diminution in virulence. Furthermore, a delay in germination (or growth) capable of causing attenuation would presumably affect pathogenesis regardless of the route of infection. To the contrary, the LD_{50} data (Table 2) indicate a major difference in the degree of attenuation depending upon the route of infection, with Δ*sod15* Δ*sodA1* Δ*sodC* Δ*sodA2* spores possessing a statistically insignificant 4.5-fold decrease in virulence via subcutaneous inoculation and more than a 40-fold attenuation via intranasal entry. This dramatic difference seems to argue against delayed germination (or growth) as the central determinant of the attenuation of Δ*sod15* Δ*sodA1* Δ*sodC* Δ*sodA2* spores and favors the importance of a factor whose role in pathogenicity is site specific. Of note, available information on the effects of germination kinetics on virulence is mixed, as certain reports indicated an increase in virulence associated with a delay in germination (35), whereas other reports showed that delayed germination attenuates virulence (32, 45).

Whereas numerous studies indicate the central role of macrophages in spore germination and dissemination in the pulmonary infectious process (15, 23, 43–45, 53), recent evidence suggests that spores inoculated subcutaneously are capable of extracellular germination and vegetative outgrowth independent of macrophages (5, 9, 10). Dormant and/or germinating spores introduced by the pulmonary route must survive interactions with ROS-generating alveolar macrophages, while macrophage-independent germination via the cutaneous route

of entry might provide a less oxidatively stressful milieu. Under the conditions found in the phagolysosomal compartment of the alveolar macrophage, the attenuation of a strain which lacks the ability to resist oxidative stress would likely be exacerbated. When seen in this way, the severe attenuation of the *sod* mutant seen via the intranasal model is explainable by the loss of a capability that cannot be properly exploited by the host when bacteria invade subcutaneously. Alternatively, given the potential differences in environmental oxygenation faced by vegetative bacilli following infection via different routes, and the growth differences and differing sensitivities of the Δ*sod15* Δ*sodA1* Δ*sodC* Δ*sodA2* mutant to endogenous oxidative stress, it is conceivable that the attenuation seen upon intranasal infection is a reflection of the oxidative stress mediated by the local host environment.

The stress protection afforded by spore-bound SODs could potentially benefit either the dormant spore or the newly germinated bacillus. While the in vitro data described in Fig. 7 and 8 measure ungerminated spores and suggest a real increase in oxidative stress sensitivity among spores of the Δ*sod15* Δ*sodA1* Δ*sodC* Δ*sodA2* strain, it remains feasible that the spore is capable of surviving concentrations of oxygen radicals and other forms of stress encountered in vivo without the benefit of SOD. In this situation, the protection afforded by SODs bound to the spore might become more important as *B. anthracis* undergoes germination within the stressful confines of the phagocytic vacuole. A previous microscopic examination of germinating spores demonstrated that the outer layers of the spore remain present and continue to envelop newly formed vegetative bacillus (24). Furthermore, it has also been shown that components of the spore are capable of conferring resistance properties to phagolysosome-bound organisms even if the two are no longer tightly associated (52). The greatest benefit of incorporating SODs into the spore may come only after *B. anthracis* begins to germinate and sheds the protective shield afforded by the total spore structure.

Available expression data (37) indicate that while *sod15* appears to undergo a sporulation-specific regulation program, *sodA1* demonstrates a high level of constitutive expression throughout all phases of the growth cycle. Thus, through distinct regulatory mechanisms, both SODs detectable within 34F2 spores appear to achieve high levels of expression within the mother cell at the time of sporulation. According to prevailing models of spore construction (7, 17, 26, 50), these high concentrations would make the proteins available for inclusion in the growing endospore. This inclusion may come about through distinct and specific protein-protein interactions occurring under the overall direction of the spore's critical morphogenetic proteins (17) or by random, nonspecific mechanics in which the highly abundant proteins are entangled in the rapidly assembling spore. Either mechanism could explain the increased spore-associated SOD activity in the Δ*sod15* Δ*sodA1* double mutant. In the event that SODs are incorporated into the spore via specific protein-protein interaction competencies, the amino acid similarity between SODs might allow for the inclusion of the remaining SODs in spaces normally occupied by SOD15 and/or SODA1. SODA2, which bears far greater similarity to both SODA1 and SOD15 than does SODC, would be better suited for such inclusion. An examination of SODs present in the SSPE generated from the various knockout constructions in this study (Fig. 6) supports this concept; the deletion of *sod15* and *sodA1* led directly to the appearance of SODA2 in the spore extract, whereas SODC was detectable only after all other SOD species had been deleted. Additionally, while both *sodA2* and *sodC* are expressed throughout the vegetative life cycle of 34F2 at relatively low levels (37), one or both genes may undergo increased levels of expression as part of a general stress response needed to cope with the loss of primary protection against oxidative stress. In this scenario, increased concentrations of SODs in the mother cell would likely facilitate greater nonspecific incorporation into the spore.

For many bacteria, redundancy among key components is important for maintaining fitness. Isozymes can provide distinct yet overlapping capabilities that allow the bacteria to thrive in multiple environmental conditions. *B. anthracis* harbors four *sod* genes, including one gene (*sodC*) putatively encoding a Cu-Zn SOD and three genes putatively encoding Mn/Fe SODs. While our work and the work of Passalacqua et al. (37) failed to find a critical role for any one SOD in an A/J or DBA/J mouse model, it is also true that mice (and humans) represent incidental hosts that make no significant contribution to the evolution and fitness of *B. anthracis*. Given the need for *B. anthracis* to survive a range of diverse hosts and environments, it is perhaps not surprising that the organism has evolved to retain such a diverse array of SODs. At the same time, the maintenance of these four genes may provide the bacteria with secondary benefits. Functional redundancy and compensation through homologous replacement are supported by previous observations of structural proteins in other *Bacillus* species (17). Regardless of the reason(s) for the persistence of multiple *sod* loci in the genome, our data suggest that the presence of four *sod* genes in the *B. anthracis* chromosome allows for compensation in the absence of one or more species. The spore-associated SOD activity (Fig. 4B) and resistance characteristics (Fig. 7B) of intermediate knockout and restorant strains carrying only a single SOD species, combined with the evidence suggesting that all SODs are capable of inclusion in the spore under the appropriate circumstances (Fig. 6), illustrate that each SOD can contribute to the properties of the spore. However, care must be taken in drawing conclusions about the relative importance of any one SOD to spore activity from data based on an evaluation of its activity in isolation because the composite level of SOD activity resident in wild-type 34F2 spores is likely dependent on several factors. These factors include, but are not limited to, the inherent specific activity of each SOD, synergistic properties between and among SODs, the concentration of each SOD within the mother cell during sporulation, and competence for the inclusion of available SOD proteins into the spore.

In conclusion, this study revealed an important role for SODs in the full virulence of *B. anthracis* Sterne in the intranasally challenged A/J mouse model. The contribution of SODs to virulence appears to reflect the protection against oxidative stress afforded the spore during the early stages of infection. We theorize that the functional redundancy created by the existence of four *sod* genes within the *B. anthracis* genome ensures that significant attenuation of the bacteria is seen only with the deletion of all four genes and the loss of spore-associated SOD activity. The sensitivity of spores to

macrophages in the absence of SODs suggests the potential therapeutic utility of small molecular inhibitors that would be capable of blocking the activity of spore-associated SOD molecules. Finally, enhanced attenuation of the Δ*sod15* Δ*sodA1* Δ*sodC* Δ*sodA2* strain seen via intranasal challenge compared to subcutaneous challenge indicates an important role for phagocyte-generated ROS in controlling anthrax infections in the lung.

ACKNOWLEDGMENTS

We thank Cara Olson for expert statistical analysis, Michael Flora for primer synthesis and DNA sequencing, and Jill Czarnecki for polyclonal antibody generation.

This work was supported by NIH/NIAID Middle Atlantic Regional Center of Excellence grant U54 AI057168 and research funds from the U.S. Navy through Uniformed Services University grant G173HS. We also give special thanks to the U.S. Army Long-Term Health Education and Training Program for support of R. Cybulski.

The opinions and assertions in this paper are the private views of the authors and are not to be construed as official or as reflecting the views of the Department of Defense. This research was conducted in compliance with the Animal Welfare Act. All animal use protocols were reviewed and approved by the Institutional Animal Care and Use Committee of the Uniformed Services University.

REFERENCES

1. **Aronson, A. I., and P. Fitz-James.** 1976. Structure and morphogenesis of the bacterial spore coat. Bacteriol. Rev. **40:**360–402.
2. **Babior, B. M., R. S. Kipnes, and J. T. Curnutte.** 1973. Biological defense mechanisms. The production by leukocytes of superoxide, a potential bactericidal agent. J. Clin. Investig. **52:**741–744.
3. **Baillie, L., S. Hibbs, P. Tsai, G. L. Cao, and G. M. Rosen.** 2005. Role of superoxide in the germination of *Bacillus anthracis* endospores. FEMS Microbiol. Lett. **245:**33–38.
4. **Bakshi, C. S., M. Malik, K. Regan, J. A. Melendez, D. W. Metzger, V. M. Pavlov, and T. J. Sellati.** 2006. Superoxide dismutase B gene (*sodB*)-deficient mutants of *Francisella tularensis* demonstrate hypersensitivity to oxidative stress and attenuated virulence. J. Bacteriol. **188:**6443–6448.
5. **Bischof, T. S., B. L. Hahn, and P. G. Sohnle.** 2007. Characteristics of spore germination in a mouse model of cutaneous anthrax. J. Infect. Dis. **195:**888–894.
6. **Brahmbhatt, T. N., B. K. Janes, E. S. Stibitz, S. C. Darnell, P. Sanz, S. B. Rasmussen, and A. D. O'Brien.** 2007. *Bacillus anthracis* exosporium protein BclA affects spore germination, interaction with extracellular matrix proteins, and hydrophobicity. Infect. Immun. **75:**5233–5239.
7. **Chada, V. G., E. A. Sanstad, R. Wang, and A. Driks.** 2003. Morphogenesis of *Bacillus* spore surfaces. J. Bacteriol. **185:**6255–6261.
8. **Chiara, M. D., F. Bedoya, and F. Sobrino.** 1989. Cyclosporin A inhibits phorbol ester-induced activation of superoxide production in resident mouse peritoneal macrophages. Biochem. J. **264:**21–26.
9. **Cote, C. K., K. M. Rea, S. L. Norris, N. Van Rooijen, and S. L. Welkos.** 2004. The use of a model of in vivo macrophage depletion to study the role of macrophages during infection with *Bacillus anthracis* spores. Microb. Pathog. **37:**169–175.
10. **Cote, C. K., N. Van Rooijen, and S. L. Welkos.** 2006. Roles of macrophages and neutrophils in the early host response to *Bacillus anthracis* spores in a mouse model of infection. Infect. Immun. **74:**469–480.
11. **Cybulski, R. J., P. Sanz, D. McDaniel, S. C. Darnell, R. L. Bull, and A. D. O'Brien.** 2008. Recombinant *Bacillus anthracis* spore proteins enhance protection of mice primed with suboptimal amounts of protective antigen. Vaccine **26:**4927–4939.
12. **Daniel, D. S., G. Dai, C. R. Singh, D. R. Lindsey, A. K. Smith, S. Dhandayuthapani, R. L. Hunter, Jr., and C. Jagannath.** 2006. The reduced bactericidal function of complement C5-deficient murine macrophages is associated with defects in the synthesis and delivery of reactive oxygen radicals to mycobacterial phagosomes. J. Immunol. **177**:4688–4698.
13. **de Benito, A. A., N. L. Padula, B. Setlow, and P. Setlow.** 2008. Sensitization of *Bacillus subtilis* spores to dry heat and desiccation by pretreatment with oxidizing agents. Lett. Appl. Microbiol. **46:**492–497.
14. **Dequeiroz, G. A., and D. F. Day.** 2008. Disinfection of *Bacillus subtilis* spore-contaminated surface materials with a sodium hypochlorite and a hydrogen peroxide-based sanitizer. Lett. Appl. Microbiol. **46:**176–180.
15. **Dixon, T. C., A. A. Fadl, T. M. Koehler, J. A. Swanson, and P. C. Hanna.** 2000. Early *Bacillus anthracis*-macrophage interactions: intracellular survival and escape. Cell. Microbiol. **2:**453–463.
16. **Dojindo Molecular Technologies.** 2004. SOD Assay Kit-WST: technical manual. Dojindo Molecular Technologies, Gaithersburg, MD.
17. **Driks, A.** 1999. *Bacillus subtilis* spore coat. Microbiol. Mol. Biol. Rev. **63:**1–20.
18. **Edwards, K. M., M. H. Cynamon, R. K. Voladri, C. C. Hager, M. S. DeStefano, K. T. Tham, D. L. Lakey, M. R. Bochan, and D. S. Kernodle.** 2001. Iron-cofactored superoxide dismutase inhibits host responses to *Mycobacterium tuberculosis*. Am. J. Respir. Crit. Care Med. **164:**2213–2219.
19. **Fang, F. C.** 2004. Antimicrobial reactive oxygen and nitrogen species: concepts and controversies. Nat. Rev. Microbiol. **2:**820–832.
20. **Fang, F. C., M. A. DeGroote, J. W. Foster, A. J. Bäumler, U. Ochsner, T. Testerman, S. Bearson, J. C. Giárd, Y. Xu, G. Campbell, and T. Laessig.** 1999. Virulent *Salmonella typhimurium* has two periplasmic Cu,Zn-superoxide dismutases. Proc. Natl. Acad. Sci. USA **96:**7502–7507.
21. **Farrant, J. L., A. Sansone, J. R. Canvin, M. J. Pallen, P. R. Langford, T. S. Wallis, G. Dougan, and J. S. Kroll.** 1997. Bacterial copper- and zinc-cofactored superoxide dismutase contributes to the pathogenesis of systemic salmonellosis. Mol. Microbiol. **25:**785–796.
22. **Gee, J. M., M. W. Valderas, M. E. Kovach, V. K. Grippe, G. T. Robertson, W. L. Ng, J. M. Richardson, M. E. Winkler, and R. M. Roop.** 2005. The *Brucella abortus* Cu,Zn superoxide dismutase is required for optimal resistance to oxidative killing by murine macrophages and wild-type virulence in experimentally infected mice. Infect. Immun. **73:**2873–2880.
23. **Guidi-Rontani, C., M. Weber-Levy, E. Labruyere, and M. Mock.** 1999. Germination of *Bacillus anthracis* spores within alveolar macrophages. Mol. Microbiol. **31:**9–17.
24. **Hachisuka, Y., K. Kojima, and T. Sato.** 1966. Fine filaments on the outside of the exosporium of *Bacillus anthracis* spores. J. Bacteriol. **91:**2382–2384.
25. **Henriques, A. O., L. R. Melsen, and C. P. Moran, Jr.** 1998. Involvement of superoxide dismutase in spore coat assembly in *Bacillus subtilis*. J. Bacteriol. **180**:2285–2291.
26. **Henriques, A. O. and C. P. Moran, Jr.** 2000. Structure and assembly of the bacterial endospore coat. Methods **20**:95–110.
27. **Janes, B. K., and S. Stibitz.** 2006. Routine markerless gene replacement in *Bacillus anthracis*. Infect. Immun. **74:**1949–1953.
28. **Kang, T. J., M. J. Fenton, M. A. Weiner, S. Hibbs, S. Basu, L. Baillie, and A. S. Cross.** 2005. Murine macrophages kill the vegetative form of *Bacillus anthracis*. Infect. Immun. **73:**7495–7501.
29. **Karavolos, M. H., M. J. Horsburgh, E. Ingham, and S. J. Foster.** 2003. Role and regulation of the superoxide dismutases of *Staphylococcus aureus*. Microbiology **149:**2749–2758.
30. **Kim, H. U., and J. M. Goepfert.** 1974. A sporulation medium for *Bacillus anthracis*. J. Appl. Bacteriol. **37:**265–267.
31. **Liu, H., N. H. Bergman, B. Thomason, S. Shallom, A. Hazen, J. Crossno, D. A. Rasko, J. Ravel, T. D. Read, S. N. Peterson, J. Yates III, and P. C. Hanna.** 2004. Formation and composition of the *Bacillus anthracis* endospore. J. Bacteriol. **186:**164–178.
32. **Lybarger, S., N. Fisher, and P. Hanna.** 2008. Spore germination: immediate early stage of anthrax. Abstr. 5th Natl. RCE Meet., Chicago, IL.
33. **Lynch, R. E., and I. Fridovich.** 1978. Effects of superoxide on the erythrocyte membrane. J. Biol. Chem. **253:**1838–1845.
34. **McCord, J. M., and I. Fridovich.** 1969. Superoxide dismutase. An enzymic function for erythrocuprein (hemocuprein). J. Biol. Chem. **244:**6049–6055.
35. **McKevitt, M. T., K. M. Bryant, S. M. Shakir, J. L. Larabee, S. R. Blanke, J. Lovchik, C. R. Lyons, and J. D. Ballard.** 2007. Effects of endogenous D-alanine synthesis and autoinhibition of *Bacillus anthracis* germination on in vitro and in vivo infections. Infect. Immun. **75:**5726–5734.
36. **Palenik, B., B. Brahamsha, F. W. Larimer, M. Land, L. Hauser, P. Chain, J. Lamerdin, W. Regala, E. E. Allen, J. McCarren, I. Paulsen, A. Dufresne, F. Partensky, E. A. Webb, and J. Waterbury.** 2003. The genome of a motile marine Synechococcus. Nature **424:**1037–1042.
37. **Passalacqua, K. D., N. H. Bergman, A. Herring-Palmer, and P. Hanna.** 2006. The superoxide dismutases of *Bacillus anthracis* do not cooperatively protect against endogenous superoxide stress. J. Bacteriol. **188:**3837–3848.
38. **Piddington, D. L., F. C. Fang, T. Laessig, A. M. Cooper, I. M. Orme, and N. A. Buchmeier.** 2001. Cu,Zn superoxide dismutase of *Mycobacterium tuberculosis* contributes to survival in activated macrophages that are generating an oxidative burst. Infect. Immun. **69:**4980–4987.
39. **Pollock, J. D., D. A. Williams, M. A. Gifford, L. L. Li, X. Du, J. Fisherman, S. H. Orkin, C. M. Doerschuk, and M. C. Dinauer.** 1995. Mouse model of X-linked chronic granulomatous disease, an inherited defect in phagocyte superoxide production. Nat. Genet. **9:**202–209.
40. **Poyart, C., E. Pellegrini, O. Gaillot, C. Boumaila, M. Baptista, and P. Trieu-Cuot.** 2001. Contribution of Mn-cofactored superoxide dismutase (SodA) to the virulence of *Streptococcus agalactiae*. Infect. Immun. **69:**5098–5106.
41. **Read, T. D., S. N. Peterson, N. Tourasse, L. W. Baillie, I. T. Paulsen, K. E. Nelson, H. Tettelin, D. E. Fouts, J. A. Eisen, S. R. Gill, E. K. Holtzapple, O. A. OKstad, E. Helgason, J. Rilstone, M. Wu, J. F. Kolonay, M. J. Beanan, R. J. Dodson, L. M. Brinkac, M. Gwinn, R. T. DeBoy, R. Madpu, S. C. Daugherty, A. S. Durkin, D. H. Haft, W. C. Nelson, J. D. Peterson, M. Pop, H. M. Khouri, D. Radune, J. L. Benton, Y. Mahamoud, L. Jiang, I. R. Hance,**

J. F. Weidman, K. J. Berry, R. D. Plaut, A. M. Wolf, K. L. Watkins, W. C. Nierman, A. Hazen, R. Cline, C. Redmond, J. E. Thwaite, O. White, S. L. Salzberg, B. Thomason, A. M. Friedlander, T. M. Koehler, P. C. Hanna, A. B. Kolsto, and C. M. Fraser. 2003. The genome sequence of *Bacillus anthracis* Ames and comparison to closely related bacteria. Nature **423:**81–86.

42. **Rose, R., B. Setlow, A. Monroe, M. Mallozzi, A. Driks, and P. Setlow.** 2007. Comparison of the properties of *Bacillus subtilis* spores made in liquid or on agar plates. J. Appl. Microbiol. **103:**691–699.
43. **Ross, J. M.** 1957. The pathogenesis of anthrax following the administration of spores by the respiratory route. J. Pathol. Bacteriol. **73:**485–494.
44. **Ruthel, G., W. J. Ribot, S. Bavari, and T. A. Hoover.** 2004. Time-lapse confocal imaging of development of *Bacillus anthracis* in macrophages. J. Infect. Dis. **189:**1313–1316.
45. **Sanz, P., L. D. Teel, F. Alem, H. M. Carvalho, S. C. Darnell, and A. D. O'Brien.** 2008. Detection of *Bacillus anthracis* spore germination in vivo by bioluminescence imaging. Infect. Immun. **76**:1036–1047.
46. **Setlow, P.** 1988. Small, acid-soluble spore proteins of *Bacillus* species: structure, synthesis, genetics, function, and degradation. Annu. Rev. Microbiol. **42:**319–338.
47. **Steichen, C., P. Chen, J. F. Kearney, and C. L. Turnbough, Jr.** 2003. Identification of the immunodominant protein and other proteins of the *Bacillus anthracis* exosporium. J. Bacteriol. **185**:1903–1910.
48. **Steinman, H. M.** 1993. Function of periplasmic copper-zinc superoxide dismutase in *Caulobacter crescentus*. J. Bacteriol. **175:**1198–1202.

48a. **Sterne, M.** 1937. Variation in *Bacillus anthracis*. Onderstepoort J. Vet. Res. **8:**271–349.

49. **Storz, G., and J. A. Imlay.** 1999. Oxidative stress. Curr. Opin. Microbiol. **2:**188–194.
50. **van Ooij, C., P. Eichenberger, and R. Losick.** 2004. Dynamic patterns of subcellular protein localization during spore coat morphogenesis in *Bacillus subtilis*. J. Bacteriol. **186:**4441–4448.
51. **Verneuil, N., A. Mazé, M. Sanguinetti, J. M. Laplace, A. Benachour, Y. Auffray, J. C. Giard, and A. Hartke.** 2006. Implication of (Mn)superoxide dismutase of *Enterococcus faecalis* in oxidative stress responses and survival inside macrophages. Microbiology **152:**2579–2589.
52. **Weaver, J., T. J. Kang, K. W. Raines, G. L. Cao, S. Hibbs, P. Tsai, L. Baillie, G. M. Rosen, and A. S. Cross.** 2007. Protective role of *Bacillus anthracis* exosporium in macrophage-mediated killing by nitric oxide. Infect. Immun. **75:**3894–3901.
53. **Welkos, S., A. Friedlander, S. Weeks, S. Little, and I. Mendelson.** 2002. In-vitro characterisation of the phagocytosis and fate of anthrax spores in macrophages and the effects of anti-PA antibody. J. Med. Microbiol. **51:**821–831.
54. **Wilks, K. E., K. L. Dunn, J. L. Farrant, K. M. Reddin, A. R. Gorringe, P. R. Langford, and J. S. Kroll.** 1998. Periplasmic superoxide dismutase in meningococcal pathogenicity. Infect. Immun. **66:**213–217.
55. **Xu, S., T. P. Labuza, and F. Diez-Gonzalez.** 2008. Inactivation kinetics of avirulent *Bacillus anthracis* spores in milk with a combination of heat and hydrogen peroxide. J. Food Prot. **71:**333–338.

Editor: F. C. Fang